Characterization of Nonlinear Switching in a Figure-of-Eight Fiber Laser Using Frequency-Resolved Optical Gating

P. G. Bollond, *Student Member, IEEE,* L. P. Barry, J. M. Dudley, R. Leonhardt, and J. D. Harvey, *Member, IEEE*

Abstract— The measurement technique of frequency-resolved optical gating is applied to determine the nonlinear switching characteristics of a passively modelocked figure-of-eight erbium-doped fiber laser. By completely characterizing the intensity and phase of the laser output pulses, the intracavity fields in the nonlinear amplifying loop mirror of the laser cavity are determined by numerical propagation using the nonlinear Schrödinger equation. Excellent switching of 95% can be achieved as a result of uniform phase characteristics developed by pulses propagating in the nonlinear amplifying loop mirror.

Index Terms—Optical fiber lasers, optical fiber switches, optical pulse generation, optical pulse measurements, ultrafast optics.

I. INTRODUCTION

THE PASSIVELY modelocked figure-of-eight fiber laser (F8L) has become an important source of picosecond pulses at a wavelength of 1.5 μm [1]. In the F8L configuration, the combination of a nonlinear amplifying loop mirror (NALM) and a linear fiber loop with an optical isolator acts as an effective saturable absorber resulting in stable modelocked operation [2]. Of particular importance to the steady-state operation of the modelocked F8L are the switching characteristics of the NALM, which are determined by the relative nonlinear phase shift induced on pulses propagating in opposite directions around the NALM, as well as linear polarization effects which occur during propagation [3]. However, although the NALM switching characteristics are well understood theoretically [2]–[4], experimental studies have been limited because of the difficulties in determining the complete characteristics of the pulses propagating in the NALM during steady-state laser operation.

In this letter, we apply the measurement technique of frequency-resolved optical gating (FROG) [5] to determine the switching characteristics of a NALM during the steady-state operation of a modelocked F8L. We use FROG measurements to determine the intensity and phase of pulses coupled out from the NALM in both the clockwise and anticlockwise directions, and using the nonlinear Schrödinger equation, we numerically propagate these pulses back into the NALM to determine the intracavity propagating fields. This allows us to study the pulse evolution within the NALM and to determine the NALM switching characteristics.
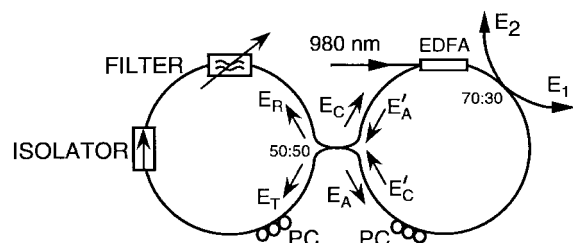
Fig. 1. Schematic diagram of the F8L used in our experiments, indicating the notation used for intracavity and output fields.

II. EXPERIMENT AND DISCUSSION

Fig. 1 shows the F8L used in our experiments. The linear loop contains a polarization-sensitive isolator to ensure unidirectional propagation, a spectral filter (FWHM $\approx$ 2 nm) for wavelength tunability, and a polarization controller (PC). The nonlinear loop contains a 5.5-m erbium-doped fiber amplifier (EDFA) pumped at 980 nm, a 27-m phase-shifting length of standard single-mode fiber (SMF) and an additional PC. The 70:30 output coupler in this F8L is positioned in the nonlinear loop immediately after the EDFA in order to study pulse propagation within the NALM [6]. At an operating wavelength of 1559 nm, stable single-pulse operation at a 4.1-MHz repetition rate is achieved at a pump power of around 10 mW. The F8L output pulses were characterized using an experimental FROG technique based on the spectral resolution of a second harmonic generation autocorrelation signal in a BBO crystal, and our experimental setup was similar to that in [5]. The pulse intensity and phase characteristics were retrieved from the measured FROG signal using standard phase-retrieval techniques [5].

Fig. 2 shows the intensity (solid line) and phase (dashed line) of the output pulses retrieved from the experimental FROG measurements. The clockwise output pulse E_1 shown in Fig. 2(a) is taken immediately after the EDFA, and the peak-power and FWHM in this case are 46 W and 1.34 ps, respectively. The figure clearly shows that the pulse E_1 has acquired an up-chirp, consistent with the effects of self-phase modulation (SPM) and normal dispersion during propagation in the EDFA. The anticlockwise output E_2 shown in Fig. 2(b) has peak-power and FWHM of 6 W and 1.70 ps, respectively, and note that the lower peak-power in this case arises since the pulse is coupled out of the cavity before the EDFA. Its propagation within the phase shifting length of the NALM is
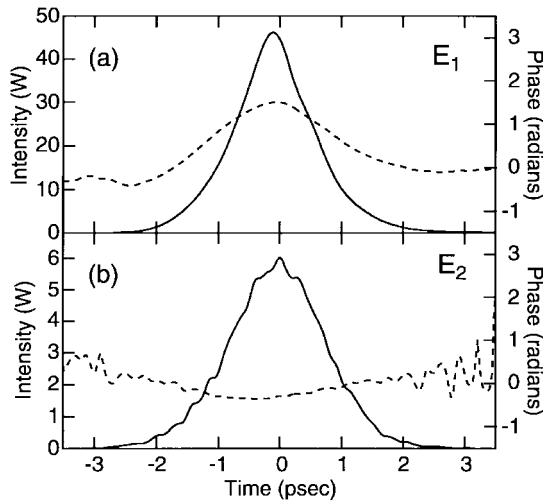
Fig. 2.   Intensity (solid line, left axis) and phase (dashed line, right axis) of (a) anticlockwise output E_1, and (b) clockwise output E_2.

therefore governed primarily by dispersion, and the phase in Fig. 2(b) clearly shows the quadratic variation from anomalous dispersion.

With complete characterization of the output fields, the intracavity fields propagating within the NALM were determined using a numerical model of pulse propagation in the output coupler and in the different fiber segments of the NALM. Because of the random birefringence of the nonpolarization preserving fiber used in the F8L, the effect of nonlinear polarization evolution is negligible and the pulses propagating within the laser experience only scalar nonlinear phaseshifts [3]. For each fiber segment, pulse propagation was, therefore, modeled using a scalar nonlinear Schrodinger equation:

$$\frac{\partial A}{\partial z} = -\frac{i\beta_2}{2}\frac{\partial^2 A}{\partial T^2} + i\gamma|A|^2 A + \frac{1}{2}g \qquad (1)$$

where $A(z,T)$ is the electric field envelope in a comoving frame, and γ and β_2 are the appropriate nonlinearity and group velocity dispersion parameters, respectively. The parameter g represents isotropic attenuation or gain in order to model propagation in standard fiber or the EDFA.

Since the parameters of standard fiber are well known, the backward-propagation of output E_2 accurately determines the anticlockwise field E_A leaving the 50:50 coupler. For standard fiber propagation, attenuation was neglected and we used $\gamma = 1.2 \times 10^{-3}$ W^{-1}·m^{-1} and $\beta_2 = -23$ ps^2/km [7]. Fig. 3(a) shows the intensity (solid line) and phase (dashed line) of the field E_A. To study the complete evolution of pulses propagating in both the clockwise and anticlockwise directions in the NALM, propagation within the EDFA must be accurately modeled, but we note that the EDFA dispersion and nonlinearity parameters are not known as accurately as for standard fiber. However, by assuming that the anticlockwise field E_A must be identical to the equivalent clockwise field E_C leaving the 50:50 coupler (within a constant phase shift of $\pi/2$ due to the coupler), the EDFA parameters can be determined using a numerical minimization technique. For some initial choice of EDFA parameters, the clockwise output E_1 is backward-propagated to obtain an estimate for field E_C,
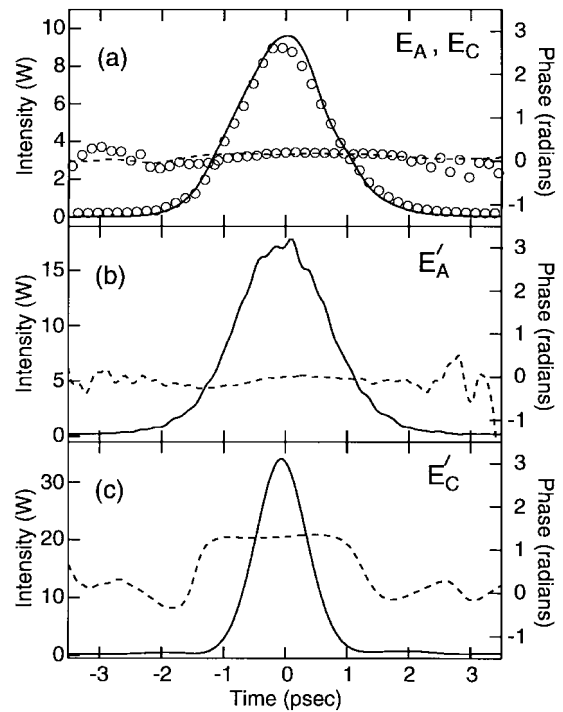

Fig. 3.   (a) Intensity (solid line, left axis) and phase (dashed line, right axis) of back-propagated pulse E_A compared with the results for pulse E_C (open circles). (b) and (c) show intensity and phase of clockwise E'_C and anticlockwise E'_A pulses incident on the 50:50 coupler.

and a numerical algorithm is used to determine the optimum parameters which minimize the error between this propagated field and the field E_A [7]. For a measured value of EDFA gain $g = 0.45$ m^{-1}, this procedure yielded EDFA parameters of $\beta_2 = +48$ ps^2/km and $\gamma = 6.0 \times 10^{-3}$ W^{-1}·m^{-1}, in good agreement with measurements of similar erbium-doped fiber [8]. The open circles in Fig. 3(a) show the intensity and phase of the optimized clockwise field E_C, and it is clear that there is very good agreement with the field E_A. Note that the $\pi/2$ difference between the phases of E_A and E_C is not shown in Fig. 3(a). It can be seen that the phase characteristics of E_A and E_C leaving the 50:50 coupler are flat, with a variation of less than 0.1 rad over the pulse FWHM. Using values for peak-power and FWHM of 9.5 W and 1.70 ps, respectively, we calculate the equivalent soliton order of the pulses E_A and E_C to be $N \sim 0.7$, implying that the pulse incident on the coupler from the linear loop of the F8L is close to a fundamental soliton.

The NALM switching characteristics were determined by the forward-propagation of the fields E_A and E_C through the NALM to yield the corresponding anti-clockwise and clockwise fields E'_A and E'_C incident on the 50:50 coupler, shown in Fig. 3(b) and (c), respectively. The intensity and phase of these fields are shown, respectively, as the solid and dashed lines in the figures. The anticlockwise field E'_A has peak-power and FWHM of 17.6 W and 1.70 ps, with a small-phase variation of 0.2 rad across the pulse FWHM. Comparion of Fig. 3(a) and (b) shows that in the anticlockwise direction, there is little evolution in the pulsewidth and phase of the initial field E_A. This is because it propagates through
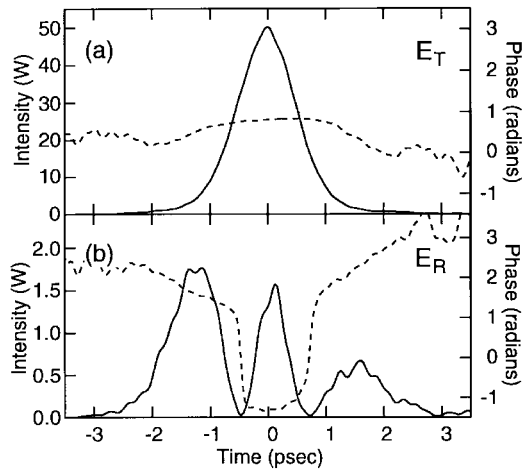
Fig. 4. Intensity (solid line, left axis) and phase (dashed line, right axis) of (a) transmitted pulse E_T and (b) reflected pulse E_R at the 50:50 coupler.

the phase-shifting length at low power before amplification in the EDFA, and is, therefore, not distorted significantly by nonlinear propagation effects. By contrast, comparing Fig. 3(a) and (c) shows that in the clockwise direction, the initial field E_C undergoes significant nonlinear evolution, because it is amplified in the EDFA immediately after leaving the 50:50 coupler, and propagates in the phase-shifting length at high power. The clockwise field E_C' has peak-power and FWHM of 38 W and 0.94 ps, respectively, and Fig. 3(c) clearly shows the effect of pulse compression and nonlinear phase distortion. Low intensity wings can be seen on the pulse, and although there is a phase shift of around 1.3 rad between the peak of the pulse and the wings, there is less than 0.1-rad variation in the phase across the pulse FWHM. This nonlinear phase evolution has been theoretically predicted to occur in a NALM as a result of soliton-like pulse evolution [3], but to our knowledge, these results are the first verification of this behavior.

The switching of the NALM occurs when the pulses E_A' and E_C' recombine in the central 50:50 coupler. The transmission of an ideal NALM can be written in the general form [3]

$$T = \tfrac{1}{2}(1 - \cos(\Delta\phi_{NL} + \Delta\phi_B)) \qquad (2)$$

where $\Delta\phi_{NL}$ is the relative nonlinear phase shift developed between the counterpropagating pulses, and $\Delta\phi_B$ is the phase bias due to the polarization controller and the loop birefrin-

gence. We have investigated the switching numerically by interfering the pulses E_A' and E_C' incident on the coupler, and our results show that optimum switching of 95% is obtained when the total relative phase shift $(\Delta\phi_{NL} + \Delta\phi_B) = \pi$, in agreement with (2). For this case, Fig. 4(a) and (b) shows the calculated transmitted and reflected fields E_T and E_R, respectively. We also note that the propagation of the trasmitted field E_T through the linear loop yields a field incident on the NALM consistent with the fields E_A and E_C obtained from the back-propagation of the experimental fields, indicating that the F8L operates close to optimum switching efficiency.

III. CONCLUSION

These FROG measurements have shown that efficient switching is achieved in a NALM even when the anticlockwise and clockwise propagating pulses have significantly different pulse durations and phase characteristics. Physically, this arises because the propagating pulses develop a relative phaseshift that is uniform over the pulse centres. The FROG technique also provides great insight into the dynamics of the F8L operation, showing in particular the presence of a fundamental soliton incident on the NALM from the linear loop of the laser.

REFERENCES

[1] I. N. Duling, III, "All fiber ring soliton laser modelocked with a nonlinear mirror," *Opt. Lett.*, vol. 16, pp. 539–541, 1991.
[2] M. Fermann, F. Haberl, M. Hofer, and H. Hochreiter, "Nonlinear amplifying loop mirror," *Opt. Lett.*, vol. 15, pp. 752–754, 1990.
[3] A. J. Stentz and R. W. Boyd, "Polarization effects and nonlinear switching in fiber figure-eight lasers," *Opt. Lett.*, vol. 19, pp. 1462–1464, 1994.
[4] I. N. Duling, III, C.-J. Chen, P. K. A. Wai, and C. R. Menyuk, "Operation of a nonlinear loop mirror in a laser cavity," *IEEE J. Quantum Electron.*, vol. 30, pp. 194–199, 1994.
[5] K. W. Delong, R. Trebino, J. Hunter, and W. E. White, "Frequency-resolved optical gating with the use of second-harmonic generation," *J. Opt. Soc. Amer. B*, vol. 11, pp. 2206–2215, 1994.
[6] W. Margulis, K. Roddwit, and J. R. Taylor, "High-power figure-of-eight laser for soliton transmission experiments," *Electron. Lett.*, vol. 31, pp. 645–646, 1995.
[7] L. P. Barry, J. M. Dudley, P. G. Bollond, J. D. Harvey, and R. Leonhardt, "Simultaneous measurement of optical fiber nonlinearity and dispersion using frequency-resolved optical gating" *Electron. Lett.*, vol. 33, pp. 707–708, 1997.
[8] B. Deutsch and Th. Pfeiffer, "Chromatic dispersion of erbium-doped silica fibers," *Electron. Lett.*, vol. 28, pp. 303–305, 1992.
[9] D. Mortimore, "Fiber loop reflectors," *J. Lightwave Technol.*, vol. 6, pp. 1217–1224, 1988.